



Published in final edited form as:

Transplantation. 2015 December ; 99(12): 2523–2533. doi:10.1097/TP.0000000000000857.

Donor Hepatic Steatosis Induce Exacerbated Ischemia-Reperfusion Injury through Activation of Innate Immune Response Molecular Pathways

Ricardo C. Gehrau¹, Valeria R. Mas¹, Catherine I. Dumur², Jihee L. Suh¹, Ashish K. Sharma¹, Helen P. Cathro³, and Daniel G. Maluf¹

Ricardo C. Gehrau: rcg2d@virginia.edu; Valeria R. Mas: vrm3n@virginia.edu; Catherine I. Dumur: cdumur@mcvh-vcu.edu; Jihee L. Suh: jls4eb@virginia.edu; Ashish K. Sharma: aks2n@cms.mail.virginia.edu; Helen P. Cathro: hpc4f@virginia.edu; Daniel G. Maluf: dgm9y@virginia.edu

¹University of Virginia, Department of Surgery, Transplant Division. P.O. Box 800625. 409 Lane Rd, Charlottesville, VA, 22908-0625, USA

²Virginia Commonwealth University, Department of Pathology. PO Box 980662, 1101 E. Marshall Street Richmond, VA 23298-0662, USA

³University of Virginia, Department of Pathology. PO Box 800904, Charlottesville, VA 22908-0214, USA

Abstract

Background—Severe liver steatosis is a known risk factor for increased ischemia-reperfusion injury (IRI) and poor outcomes post liver transplantation (LT). This study aimed to identify steatosis-related molecular mechanisms associated with IRI exacerbation post-LT.

Methods—Paired graft biopsies (n=60) were collected at pre-implantation (L1) and 90 min post-reperfusion (L2). LT recipients (n=30) were classified by graft macrosteatosis: without steatosis or 5% (WS, n=13) and with steatosis 25% (S, n=17). Plasma samples were collected at L1, L2, and 1-day post-LT (POD1) for cytokines evaluation. Tissue RNA was isolated for gene expression microarrays. Probeset summaries were obtained using RMA algorithm. Pairwise comparisons were fit using two-sample *t*-test. *P*-values < 0.01 were significant (FDR < 5%). Molecular pathway analyses were conducted using IPA tool.

Results—Significantly differentially expressed genes were identified for WS and S grafts, post-reperfusion. Comprehensive comparison analysis of molecular profiles revealed significant association of S grafts molecular profile with innate immune response activation, macrophages production of nitric oxide and reactive oxygen species, IL-6, IL-8, IL-10 signaling activation,

Corresponding author: Daniel G. Maluf, MD, Surgical Director Liver Transplantation, University of Virginia, Department of Surgery. 1300 Jefferson Park Av. Barringer 5, room 5417. Charlottesville, VA, 22908- 0708, USA, dgm9y@virginia.edu.

Disclosure: The authors declare no conflicts of interest.

Author's specific contributions:

Participated in research design: VRM, DGM, RCG

Participated in the writing of the paper: RCG, VRM, DGM

Participated in the performance of the research: RCG, JLS, VRM, DGM

Contributed new reagents or analytic tools: HPC, AKS, VRM, DGM

Participated in data analysis: RCG, CID, VRM

recruitment of granulocytes, and accumulation of myeloid cells. Post-reperfusion histological patterns of S grafts revealed neutrophilic infiltration surrounding fat accumulation. Circulating pro-inflammatory cytokines at post-reperfusion and 24 hours post-LT concurred with intra-graft deregulated molecular pathways. All tested cytokines were significantly increased in plasma of S grafts recipients at post-reperfusion when compared with WS group at same time.

Conclusions—Increases of graft steatosis exacerbate IRI by exacerbation of innate immune response post-LT. Preemptive strategies should consider it for safety usage of steatotic livers.

INTRODUCTION

Liver transplantation (LT) remains the most effective treatment option for end stage liver disease (1). However, wider application of LT is limited by organ shortage (2,3). This issue had led to a more aggressive acceptance and usage of liver grafts from extended criteria donors (ECD) (3,4). While the use of ECD livers predispose to initial poor function, the usage of these grafts demonstrated acceptable outcomes and decreased waitlist time and mortality rates (5,6).

Despite that moderate-to-severe liver donor steatosis (more than 30%-60% graft macrosteatosis) has been associated with poor patient and graft outcome (7,8), graft steatosis is not usually included as risk variable in current used organ donor prognostic models such as donor risk index (DRI) (9). There is intensive ongoing research aiming to identify new pre-conditioning strategies for diminishing adverse effects of allograft steatosis post-LT (10–15). Specifically, new therapies tested in murine models demonstrated effective decreasing of inflammatory response and parenchymal damage as major consequences of exacerbated ischemia-reperfusion injury (IRI) in steatotic liver grafts (10). Similarly, promising strategies are under investigation with normothermic (37°C) and subnormothermic mechanic perfusion to induce graft defatting and minimize IRI (11,12). Furthermore, the addition of different agents to the University of Wisconsin solution, such as proteasome inhibitors (Bortezomib) (13), alpha/beta blockers (Carvedilol) (14), or growth factors (EGF/IGF-I) (15) demonstrated outcome's improvements for steatotic livers.

IRI is a multifactorial process characterized by an oxidative stress scenario and the release of a pro-inflammatory cytokines after activation of innate immune response, which then triggers influx of inflammatory activated cells (16–19). However, molecular mechanisms of IRI and the interconnection between outcomes and graft steatosis in LT are not well-documented. In this regard, lipids accumulation within the hepatic parenchyma of the graft seems to strengthen this pro-inflammatory scenario (20). Several deleterious mechanisms had being proposed including excessive lipid peroxidation, which contribute to an exuberant inflammatory response, architectural alteration of microvessel structure that decrease sinusoidal blood flow converging to energy depletion, and mitochondrial dysfunction favoring necrosis instead of apoptosis (20). Blockade of certain signaling pathways including complement and toll-like receptor 4 (TLR4) reduced IRI levels in steatotic allografts, therefore postulating these as major molecular exacerbating effectors (21,22). However, the effect of fat droplet accumulation in hepatocytes on IRI-related molecular and cellular pathways is not clear yet.

Hereby, this study aimed to identify key molecular mechanisms and pathways deregulated post-reperfusion and associated with exacerbation of IRI in steatotic human liver grafts.

MATERIALS AND METHODS

Patients and biopsy samples

The Institutional Review Board at the University of Virginia approved this study (IRB-HSR# 15986). Written informed consent forms were obtained from all participants. In total, 30 cases out of 107 consecutive LT procedures were selected for the study based on available biopsy samples with histological evaluation for steatosis before implantation and were transplanted. Steatosis (macrosteatosis) severity were determined in both liver lobes and reported as average value. No liver allografts were discarded based solely on steatosis at time of transplantation. For study purpose, LT recipients were classified according with allograft macrosteatosis grade as: (1) without steatosis (WS, n = 13), including allografts with steatosis / macrosteatosis (<5%), and (2) with steatosis (S, n = 17) including allografts with steatosis / macrosteatosis \geq 25%. Paired liver allograft biopsy samples were obtained at pre-implantation (L1) and at 90 minutes post-reperfusion (L2), and collected in RNAlater™ reagent (Ambion Inc., Austin, TX, USA) following storage at -80°C until use.

RNA isolation and gene expression microarrays

Total RNA was isolated from liver biopsy samples using Trizol. Quality control (QC) evaluation for RNA purity and integrity were performed in accordance with previous established criteria (23). All RNA samples met QC and were then used for messenger RNA (mRNA) labeling followed by Affymetrix™ HG-U133A v2.0 GeneChip® microarrays hybridization (n = 50). Hybridized microarrays were scanned on an Affymetrix GeneChip® Scanner 3000 G7. Probe set intensity raw data were electronically stored in .DAT and .CEL files using GeneChip® Operating Software (GCOS).

Statistical analysis and biological interpretation

Gene expression GeneChip microarray QC and normalization procedures followed previous established parameters (24,25). Probeset summaries were obtained using RMA algorithm. For statistical purposes, all available probesets (n = 22,277) were included for gene expression analysis to rule out significant differences for control probesets. Pairwise comparisons between L1 vs. L2 for WS and S study groups were fit using two-sample *t*-test in R environment (26). A *p*-value \leq 0.01 was considered as significant by controlling a False Discovery Rate (FDR) lower than 5% and 1% for WS group and S group, respectively, estimated using Benjamini and Hochberg method (27). Fold-change values were used for differential expression trend and magnitude estimation.

Biological interpretation

Ingenuity Pathway Analysis (IPA) software (www.ingenuity.com) was used for gene ontology and pathway analyses, and core analysis comparison. Genes identified as significantly differentially expressed between L1 vs. L2 in each study group were uploaded to IPA software in spreadsheet work lists containing probeset IDs and fold-changes. A *p*-value \leq 0.05 was considered significant. IPA generated activation z-score (z) was used for

molecular pathways and cellular functions activity interpretation as described in a previous study (28).

Real time PCR validation

We selected genes for validation studies were based on significance, biological role, and deregulation magnitude (fold-change). RNA reverse transcription reactions were performed using TaqMan[®] gene expression reverse transcription reagents (Applied Biosystems, CA, USA). Gene expression validation analyses were conducted using Taqman[®] qPCR assays (assay ID) for target genes *CH25H* (Hs02379634_s1), *EGR3* (Hs00231780_m1), *SOCS3* (Hs02330328_s1), *CCL2* (Hs00234140_m1), and *TNFAIP6* (Hs01113602_m1). *GAPDH* (Hs99999905_m1) was used as endogenous control (standard). Expression analysis was performed using delta-Ct model (mean Ct_{target} - mean Ct_{standard}). *P*-values < 0.05 were considered significant.

Histological evaluation

Hematoxylin and Eosin (H&E) dyed sections from formalin-fixed and paraffin-embedded liver allograft biopsy samples collected at post-reperfusion were examined by an experienced pathologist (HPC).

Plasma samples collection and cytokine measurements

Whole peripheral blood samples were drawn using EDTA as anticoagulant from all included LT recipients at pre-implantation (L1), at 90 min post-reperfusion (L2), and at 24 hours post LT or post-operative day 1 (POD1). Plasma was obtained by blood centrifugation. Cytokine concentrations were measured using a multiplex bead array technique (Bio-Plex Pro[™] Human Chemokine Assay; Bio-Rad Laboratories, Hercules, CA) following manufacturer's instructions using Bio-Plex 200 System (Bio-Rad, Hercules, CA). Selection criteria of cytokines corresponded with observed gene expression and molecular pathways from biopsies.

RESULTS

Patients and clinical parameters

Written informed consents were obtained from all LT recipients. From a total of 103 consecutive deceased donor liver transplant cases, 30 donor organs representing the extreme steatotic grades (group S (n = 17; macrosteatosis 25%) and group WS (n = 13; macrosteatosis <5%)), were selected for the study. Demographics and clinical variables for donors-recipients, and preservation methods were homogeneously distributed between groups (Table 1A). Cause of liver disease and donor-recipient demographic and clinical characteristics are described in Table 1A. Patients from both study groups showed similar hospital length-of-stay (LOS) but patient survival was lower in LT recipients of the S group (Table 1A). As described in Table 1B, serum transaminases were significantly higher in the S group with AST activity increased almost 5- and 3-fold-changes at post-reperfusion (90 min) and at POD1, respectively, while it remained similar up to 1-month post-LT compared with WS group. Similarly, ALT activity was significantly increased at post-reperfusion, POD1, and POD7, while remaining no significantly increased at 1-month post-surgery.

Coagulation parameters were similar between groups and total bilirubin remained increased but no significant in the S group up to 1-month of follow-up (Table 1B).

Differentially expressed molecular profiles

Pairwise comparison analyses were performed between L1 samples for each study group (L1-S vs. L1-WS), where no significant differentially expressed genes were observed (FDR 5%).

Gene expression analysis between L1 vs. L2 for each group identified significantly differentially expressed genes for S (1,264 genes) and WS (350 genes) groups (Fig. 1A). Both expression profiles shared 231 genes (135 upregulated and 96 downregulated) (Fig. 1A and Supplementary Table S1). Analysis of differential expression magnitudes (L1 vs. L2; fold-changes - FC) between groups identified 11 common genes (*CCL20*, *CXCL8*, *MAFF*, *BIRC3*, *RND1*, *CXCL1*, *SLC2A3*, *PTGS2*, *BCL2A1*, *CXCL3*, and *ICAM1*) with increased expression of at least 1.5 fold-changes in S group (Supplementary Table S1). Importantly, pro-inflammatory cytokines encoding genes *CCL20*, *CXCL8*, and *CXCL1* were significantly overexpressed in S group (ANOVA, $p = 0.001$; $p < 0.001$; and $p = 0.016$, respectively) together with *BIRC3* ($p = 0.005$) gene.

Gene ontology and pathway analyses were conducted to biologically interpret common and unique gene expression profiles between study groups. In total, 318 molecular pathways were significantly ($p < 0.05$) associated with common deregulated genes between S and WS groups post-reperfusion (Supplementary Table S2). Top ten canonical pathways were significantly involved in activation and function of innate immune-related cells and pro-inflammatory molecular signaling pathways regulation (Fig. 1B). Importantly, almost all genes involved in those pathways were significantly upregulated post-reperfusion (Supplementary Figure S1). Predicted activation z-score values were assigned for 55 significant canonical pathways. Of those, 22 molecular pathways were predicted as significantly activated ($z \geq 2.0$). In contrast, peroxisome proliferator-activated receptor (PPAR) signaling pathway was predicted as inhibited ($z = -2.3$), which is in accordance with up-regulation of genes encoding for interleukin-1B (*IL1B*) and its receptor antagonist (*IL1RN*), *JUN*, *FOS*, *KRAS*, *NFKBIA*, *PPARD*, and *PTGS2*, as well as activation and pro-inflammatory cytokines signaling pathways (Fig. 1C and Supplementary Table S1). Unique genes from WS group were significantly associated with molecular pathways involved in decreases transmembrane potential of mitochondria and mitochondrial membrane ($p = 0.019$), increases damage of mitochondria ($p = 0.050$), and decreases respiration of mitochondria ($p = 0.050$). Interestingly, S group unique genes were significantly related to p53 signaling ($p = 1.2E10^{-5}$), RAR activation ($p = 1.4E10^{-3}$), LXR/RXR activation ($p = 1.7E10^{-3}$) and HIF signaling ($p = 4.8E^{-3}$) among the top 5 more significant molecular pathways (Fig. 1D). However, most highly upregulated significant genes including *CH25H* (8.6-fold change; $p = 7.7E^{-8}$), *CALCA* (7.8-fold change; $p = 2.6E^{-6}$), *FOSB* (5.5-fold change; $p = 1.5E^{-5}$), *CCL2* (5.3-fold change; $p = 1.1E^{-5}$), *PHLDA2* (4.8-fold change; $p = 4.9E^{-6}$), *EGR3* (4.5-fold change; $p = 3.8E^{-5}$), *TNFAIP6* (4.3-fold change; $p = 9.9E^{-5}$), *EMPI* (3.7-fold change; $p = 2.5E^{-5}$), and *SOCS3* (3.5-fold change; $p = 5.6E^{-8}$) encode for critical molecules expressed in and positive regulators of monocytes / macrophages and

lymphocytes activation functions. In addition, 24 associated network functions (score value > 20) were identified for S group unique genes. Top ten networks were associated with connective tissue disorders (networks 1, 6 and 10) and specially with cellular processes involved in cell morphology (networks 6 and 7), tissue development (network 2), and DNA repair and RNA transport (networks 9 and 10) (Table 2A). Unique genes from WS livers were included in 8 associated network functions preferentially involved in connective tissue development and function, and cellular development, growth, and proliferation (Table 2B).

These findings elucidate common molecular mechanisms associated with steatosis and IRI between groups. However, these observations also suggest increases of innate immune response and cellular damage and repair in steatotic livers post-reperfusion.

Comparison analysis for comprehensive biological interpretation

To better comprehend the impact of increased steatosis on IRI, deregulated molecular profiles from S and WS groups were individually analyzed (L1 vs. L2 for each group) for comparative biological interpretation. Predicted activity of molecular pathways and biological functions were considered significant according p -values less than 0.05 estimated by IPA. Molecular pathway analyses were focused mainly on pro-inflammatory and immune response signaling. As illustrated in Figure 2, the role of innate immune response cells (macrophages) from the analysis of inflammatory diseases canonical pathway was more significant in S group ($p = 1.2E-10$) vs. WS group ($p = 5.5E-06$). In a same trend, signaling cascades for nitric oxide and ROS production in macrophages were more significantly associated with steatotic grafts (S group $p = 2.0E-05$ vs. WS group $p = 2.5E-03$). It was accompanied by increased significance of pro-inflammatory signaling cascades for IL-6 ($p = 6.4E-09$ vs. $p = 1.8E-06$), IL-8 ($p = 2.2E-05$ vs. $p = 2.2E-03$), and IL-10 ($p = 1.0E-05$ vs. $p = 1.2E-02$) signaling cascades in S group vs. WS group (Fig. 2).

The top significant canonical pathway was further analyzed between groups (Supplementary Figure S2). Functional activation analysis predicted recruiting, infiltration, and activation of leukocytes independently of steatosis grade. However, pro-inflammatory cytokines and adhesion molecules encoding genes (*IL-1*, *IL-6*, *IL-8*, *ICAM-1*, and *MCP-1*) demonstrated increased expression in S group (Supplementary Figure S2A) in comparison with the WS group (Supplementary Figure S2B), which of those *IL-1* and *IL-8* encoding genes demonstrated significant increase expression, previously represented by the common genes expression analysis mentioned above. These results are in good agreement with previous analyses of unique genes from each molecular profile as mentioned above. Therefore, these observations may also suggest increased innate immune response and pro-inflammatory activity triggered in steatotic liver allografts post-reperfusion.

Predicted activity of molecular and cellular functions post-reperfusion

Molecular and cellular functions were analyzed to determine significant predicted activity using z scores ($z \geq 2.0$) estimated from IPA tool. The analysis was restricted to inflammatory and immune related functions. The analysis identified 39 cellular and molecular functions predicted as significantly activated. In total, 6 functions were specific for S group, 11 for WS group, and 22 biological functions were shared between groups

(Table 3). S group specific functions were involved in recruitment of granulocytes ($z = 3.0$) and blood cells ($z = 3.5$), and accumulation of myeloid cells ($z = 2.4$). In contrast, biological functions specific for WS group were associated with molecular networks involved in adaptive immune response, which include as most relevant movement ($z = 3.5$) and recruitment ($z = 2.1$) of lymphocytes, activation ($z = 3.4$) and recruitment ($z = 2.2$) of antigen presenting cells, migration of phagocytes ($z = 2.5$).

The molecular profile from S group predicted increased significance in homing of cells ($z = 3.6$) compared with WS group ($z = 2.9$). Interestingly, WS grafts associated profile predicted increased activation of phagocytes ($z = 3.4$) compared with S group ($z = 2.6$) despite both profiles revealed similar phagocytes recruitment activity (S group, $z = 3.2$; WS group, $z = 2.9$), as well as recruitment of leukocytes and neutrophils (Table 3). In spite of predicted as activated in both groups, cellular functions involved in differentiation of blood cells, activation, differentiation, and homeostasis of leukocytes, development and homeostasis of lymphocytes, and T cell homeostasis and development were significantly predicted as associated in allografts from WS group post-reperfusion (Table 3).

Gene expression validation analysis

Five selected genes (*CH25H*, *EGR3*, *SOCS3*, *CCL2*, and *TNFAIP6*) associated with S group were successfully validated by RT-qPCR assays as shown in Table 4. Expression trends and significance demonstrated to be similar to gene expression microarray results for these selected molecules.

Pro-inflammatory cellular infiltrates post-reperfusion

Histological evaluation post-reperfusion biopsies post-reperfusion determined pro-inflammatory neutrophilic infiltrates with different pattern between groups. Non-steatotic allografts showed pro-inflammatory infiltrates confined to the peripheral area of portal spaces (Fig. 3A). In steatotic livers, neutrophilic pro-inflammatory cellular infiltrates were majorly observed directly surrounding hepatocytes accumulating lipids (Fig. 3B).

Circulating cytokines and chemokines

Circulating concentrations of selected pro-inflammatory cytokines were analyzed at post-reperfusion (90 min) and 24 hours post-surgery and compared against pre-implantation levels for each study group (Fig. 4). From the analysis, all tested cytokines were found significantly increased in S group allografts at post-reperfusion. Interestingly, concentrations for IL-1 β , IL-2, IL-4, IL-6, IL-8, CCL20, MCP-1, and TNF- α were also significantly elevated at 24 hours or POD1 in comparison with pre-implantation levels. However, only concentration levels for IL-6, IL-8, IL-10 and MCP-1 were significantly increased in WS allografts at post-reperfusion (Fig. 4).

Cytokines levels were also compared at each time-point between study groups (Table 5). From the analysis, no significant differences in concentration levels were encountered at pre-LT between groups for all tested cytokines. However, all cytokines revealed significant increased concentrations in S group plasma samples at post-reperfusion in comparison with WS group at the same time-point. Similarly, IL-1 β , IL-4, IL-6, IL-8, CCL20, TNF- α , and

CXCL-1 demonstrated significant increased levels in S group samples *versus* WS group at POD1 (Table 5).

Importantly, significant increases of circulating levels for IL-1 β , IL-6, IL-8, CCL20, MCP-1, CXCL-1, and TNF- α in steatotic livers at post-reperfusion corresponded with molecular expression profiles for each cytokine encoding genes in S group L2 biopsy samples.

DISCUSSION

Steatotic livers exhibit elevated intrahepatic triglyceride (TG) levels in the form of large lipid droplets (LDs), reduced adenosine triphosphate (ATP) levels, and elevated reactive oxygen species (ROS) levels, factors that contribute to their elevated sensitivity to IRI during transplantation (29). Moderate to severe steatosis is considered an independent risk factor for worse outcome post-LT (7,30–32). However, several authors reported safety usage of moderate steatotic livers (33–35), and living donation (36–38). Nevertheless, usage of steatotic liver grafts are possible along with minimization of other donor / graft and recipient risk factors such as long cold ischemia time and high MELD scores (7,32,33,39). Outcome results from the current study are comparable with others (Table 1).

Chavin *et al.*, (33) demonstrated increased transaminases activity and slower restoration of coagulation activity in LT recipients of steatotic allografts though no extending hospital LOS or reducing survival rates. This biochemical scenario was attributed to an increased sensitivity to IRI, as also previously reported (36). Major efforts are conducted to minimize tissue damage at transplant time by either surgical maneuvers and drugs therapy (10–15,40,41). Molecular mechanisms underlying IRI exacerbation in steatotic livers deserve a comprehensive understanding to accelerate the progress of ongoing therapeutic strategies.

To the best of our knowledge, this is the first study to analyze at the molecular level the impact of graft steatosis in IRI. This study suggests differential regulation of pro-inflammatory and immune response molecular profiles associated with IRI in steatotic livers. More specifically, increased activation of innate immune response molecular pathways corresponded with higher level of pro-inflammatory response post-reperfusion. It is also supported by the activation of molecular pathways involved in macrophages reaction and production of ROS in addition to increased significance of pro-inflammatory cytokines signaling pathways (IL-1, IL-6, and IL-8), proliferation of connective tissue cells, and cell/tissue damage (e.g. p53-signaling). Despite activation of pro-inflammatory molecular pathways in non-steatotic livers, these were majorly involved in recruitment, activation, and development of lymphocytes, as well as antigen presentation cells. IRI molecular pathways and mechanisms associated with LT were previously characterized by our group using data integration analysis (28). Interestingly, we observed similar predicted activation profiles of cellular functions and increased homeostasis of lymphocytes for WS livers. However, activation and/or exacerbation of innate immune response related molecular pathways suggest being a prevalent and augmented feature in IRI associated with severe steatosis in LT.

Independently of allograft type, macrophages accumulation and activation occur within the early phase of IRI processes triggering quick and intense innate immune response activation and organ injury (42). Moreover, through the production of pro-inflammatory mediator and its capacity as antigen presenting cells, accumulated macrophages may promote adaptive T cell response (18,42). Previous studies demonstrated increased activity of Kupffer cells (KC), the hepatic macrophage, in steatotic liver allografts (17). Together with sinusoidal endothelial cells (SECs), KCs demonstrated to be crucial for an oxidative stress and pro-inflammatory scenario set up by releasing reactive oxygen species (ROS) and pro-inflammatory cytokines (TNF- α , IL-1, and IL-6) during the IRI early phase, upon activation induced through TLR4 signaling (16–18,43). ROS scavenging mechanisms (superoxide dismutases) represent candidates for therapeutic interventions to minimize oxidative stress (29). However, the TLR4 signaling pathway is essential for macrophage activation, and its deficiency demonstrated protective effects for IRI injury basically involving reduced levels of TNF- α and IL-6 cytokines (42,44,45). In addition, activation of TLR4 signaling induces adaptive response by increasing CD4 cells infiltration constantly sustained as demonstrated in murine models (22). From our results, histological evaluation of liver allografts revealed neutrophilic infiltration surrounding fat areas in steatotic allografts while portal accumulation in non-steatotic livers at post-reperfusion. It suggests a focal pro-inflammatory response induced by fat accumulation in hepatocytes denoted by specific distribution of cellular infiltrate patterns post-reperfusion. Overall, concentrations of circulating pro-inflammatory cytokines were significantly increased in steatotic graft LT recipients at post-reperfusion, and at 24 hours post-surgery. These findings positively correlated with further activated pro-inflammatory signaling cascades (e.g. IL-1, IL-6, and TNF- α) observed at molecular level in steatotic liver tissues. Together with predicted significantly increased role on macrophages and production of ROS and nitric oxide suggest that steatotic liver allografts are prone to suffer increased tissue injury associated with exacerbation of innate immune response mechanisms.

Increment of lipid peroxidation is also associated with steatosis and well-represent an extra source for ROS production consequently contributing to increased IRI (29,30). In particular, this phenomenon may be also attributed to cholesterol accumulation in mitochondria. The reported study from Llacuna *et al.*, (46) characterized enhanced IRI associated with mitochondrial depolarization and ROS production when cholesterol accumulates in mitochondria, and it directly correlated with increases in steroidogenic acute regulatory protein (StAR), which is a mitochondrial cholesterol transporting polypeptide, and Glutathione depletion. Interestingly, specific inhibitors of cholesterol synthesis pathway ameliorated mitochondrial cholesterol deposition, perhaps inhibiting the *de novo* synthesis, plus protecting against IRI (46). From our results, the expression of the cholesterol-25-hydroxylase enzyme encoding gene (*CH25H*) was found as top significantly increased (8.6-fold changes; $p = 7.7E-08$) in allografts from the S group and further validated by RT-qPCR. The *CH25H* gene expression was demonstrated to be dependent of TLR4 signaling by treatment with LPS (TLR4 ligand), which induce increment of 25-hydroxycholesterol concentration in macrophages (47). More interestingly, 25-hydroxycholesterol was identified as a natural booster of the inflammatory signaling in macrophages by modulating the transcriptional regulation of TLR-responsive genes via AP-1 (48), a central

transcriptional event in hepatic IRI (17,18). Although it may represent only a small part of the puzzle, and deserve further cellular and molecular mechanistic characterization, steatosis via cholesterol may induce superlative oxidative stress levels originated from activated KC that provoke higher levels of pro-inflammatory cytokines.

Prolonged cold-ischemia time (CIT) demonstrated to be an additive threat for IRI severity in steatotic livers. Spitzer *et al.*, (7) identified a direct interaction between macrosteatosis and extended CIT (> 11 hours) with poor graft function. Deroose *et al.*, (49) demonstrated significant correlation between prolonged CIT, severe steatosis (>60%), and DCD with allograft dysfunction. In our series, CIT was comparable between groups and no DCD grafts were included.

Hereby, our experimental data suggest that graft steatosis exacerbates IRI mechanisms and induces increased innate immune response. It further correlated with significant increases of transaminases activity post-reperfusion, and during 1-week post-LT preferentially for ALT activity, as well as histology observations and increased concentrations of pro-inflammatory cells post reperfusion. Previous studies also shown higher peaks of serum transaminases activity with slower decline in steatotic livers (33,35,49,50). Interestingly, in most of those reports, and only in accordance with reported AST activities from the current study, serum transaminases activity values were similar at 1-week post-LT between steatotic and non-steatotic liver recipients. Also, in our study, the S group LT recipients showed increased though not significant total bilirubin at 1-week post-LT. Despite lower survival rates may be due to small sample size, liver allograft function looks comparable with non-steatotic livers after 1-week post-surgery, which is in agreement with previous reports (30,31,33,35,51). Nevertheless, this issue needs further evaluation in large patient cohorts.

Relevant evidence from histological biopsy assessment and non-invasive new imaging technology demonstrated that allograft steatosis may quickly decrease after 2-weeks post-LT, reaching normal rates at 18-month post-surgery (38,51,52). In agreement with reports from Neuberger *et al.*, (30) and Chavin *et al.*, (33), steatotic allograft LT recipients might achieve acceptable long-term outcomes. Liver defatting (20), ischemic preconditioning (40), subnormothermic perfusion (11,53), drugs aimed to eliminate toxic substances (e.g. ROS) from the hepatic microenvironment (29,41,54), and even diet-treated liver steatotic donors for living donation (55) are major potential strategies, to reduce the steatotic burden decreasing the mentioned effect on IRI.

In conclusion, graft steatosis prompt IRI exacerbation by promoting increases in innate immune response reflected by a stronger pro-inflammatory response. Development of interventional treatments targeting molecular pathways involved in innate response cellular activation may help to reduce the additive IRI injury effect in steatotic allografts.

Supplementary Material

Refer to Web version on PubMed Central for supplementary material.

ABBREVIATIONS

CIT	Cold-ischemia time
DCD	Donation after cardiac-arrest
DRI	Donor Risk Index
FDR	False discovery rate
GCOS	Genechip operating software
ICU	Intensive care unit
IPA	Ingenuity Pathway Analysis
IR	Ischemia reperfusion
IRB	Institutional review board
LOS	Hospital Length-of-Stay
LT	Liver transplantation
NS	No steatosis
QC	Quality control
RMA	Robust Multi-array Average
RNA	Ribonucleic acid
ROS	Reactive oxygen species
WIT	Warm ischemia time
WS	With steatosis

REFERENCES

1. Dienstag JL, Cosimi AB. Liver transplantation--a vision realized. *N.Engl.J.Med.* 2012; 367:1483. [PubMed: 22992048]
2. Kim WR, Smith JM, Skeans MA, et al. OPTN/SRTR 2012 Annual Data Report: liver. *Am.J.Transplant.* 2014; 14(Suppl 1):69. [PubMed: 24373168]
3. Wertheim JA, Petrowsky H, Saab S, Kupiec-Weglinski JW, Busuttil RW. Major challenges limiting liver transplantation in the United States. *Am.J.Transplant.* 2011; 11:1773. [PubMed: 21672146]
4. Attia M, Silva MA, Mirza DF. The marginal liver donor--an update. *Transpl.Int.* 2008; 21:713. [PubMed: 18492121]
5. Barshes NR, Horwitz IB, Franzini L, Vierling JM, Goss JA. Waitlist mortality decreases with increased use of extended criteria donor liver grafts at adult liver transplant centers. *Am.J.Transplant.* 2007; 7:1265. [PubMed: 17359503]
6. Tector AJ, Mangus RS, Chestovich P, et al. Use of extended criteria livers decreases wait time for liver transplantation without adversely impacting posttransplant survival. *Ann.Surg.* 2006; 244:439. [PubMed: 16926570]
7. Spitzer AL, Lao OB, Dick AA, et al. The biopsied donor liver: incorporating macrosteatosis into high-risk donor assessment. *Liver Transpl.* 2010; 16:874. [PubMed: 20583086]
8. de Graaf EL, Kench J, Dilworth P, et al. Grade of deceased donor liver macrovesicular steatosis impacts graft and recipient outcomes more than the Donor Risk Index. *J.Gastroenterol.Hepatol.* 2012; 27:540. [PubMed: 21777274]

9. Feng S, Goodrich NP, Bragg-Gresham JL, et al. Characteristics associated with liver graft failure: the concept of a donor risk index. *Am.J.Transplant.* 2006; 6:783. [PubMed: 16539636]
10. von Heesen M, Seibert K, Hulser M, et al. Multidrug donor preconditioning protects steatotic liver grafts against ischemia-reperfusion injury. *Am.J.Surg.* 2012; 203:168. [PubMed: 21782153]
11. Liu Q, Berendsen T, Izamis ML, Uygun B, Yarmush ML, Uygun K. Perfusion defatting at subnormothermic temperatures in steatotic rat livers. *Transplant.Proc.* 2013; 45:3209. [PubMed: 24182786]
12. Jamieson RW, Zilvetti M, Roy D, et al. Hepatic steatosis and normothermic perfusion-preliminary experiments in a porcine model. *Transplantation.* 2011; 92:289. [PubMed: 21681143]
13. Zaouali MA, Bardag-Gorce F, Carbonell T, et al. Proteasome inhibitors protect the steatotic and non-steatotic liver graft against cold ischemia reperfusion injury. *Exp.Mol.Pathol.* 2013; 94:352. [PubMed: 23305864]
14. Ben Mosbah I, Rosello-Catafau J, Alfany-Fernandez I, et al. Addition of carvedilol to University Wisconsin solution improves rat steatotic and nonsteatotic liver preservation. *Liver Transpl.* 2010; 16:163. [PubMed: 20104484]
15. Zaouali MA, Padrissa-Altes S, Ben Mosbah I, et al. Improved rat steatotic and nonsteatotic liver preservation by the addition of epidermal growth factor and insulin-like growth factor-I to University of Wisconsin solution. *Liver Transpl.* 2010; 16:1098. [PubMed: 20818748]
16. Bahde R, Spiegel HU. Hepatic ischaemia-reperfusion injury from bench to bedside. *Br.J.Surg.* 2010; 97:1461. [PubMed: 20645395]
17. de Rougemont O, Dutkowski P, Clavien PA. Biological modulation of liver ischemia-reperfusion injury. *Curr.Opin.Organ.Transplant.* 2010; 15:183. [PubMed: 20125019]
18. Zhai Y, Busuttill RW, Kupiec-Weglinski JW. Liver ischemia and reperfusion injury: new insights into mechanisms of innate-adaptive immune-mediated tissue inflammation. *Am.J.Transplant.* 2011; 11:1563. [PubMed: 21668640]
19. Eltzschig HK, Eckle T. Ischemia and reperfusion--from mechanism to translation. *Nat.Med.* 2011; 17:1391. [PubMed: 22064429]
20. Nativ NI, Maguire TJ, Yarmush G, et al. Liver defatting: an alternative approach to enable steatotic liver transplantation. *Am.J.Transplant.* 2012; 12:3176. [PubMed: 23057797]
21. He S, Atkinson C, Evans Z, et al. A role for complement in the enhanced susceptibility of steatotic livers to ischemia and reperfusion injury. *J.Immunol.* 2009; 183:4764. [PubMed: 19752222]
22. Ellett JD, Evans ZP, Atkinson C, Schmidt MG, Schnellmann RG, Chavin KD. Toll-like receptor 4 is a key mediator of murine steatotic liver warm ischemia/reperfusion injury. *Liver Transpl.* 2009; 15:1101. [PubMed: 19718644]
23. Mas VR, Maluf DG, Stravitz R, et al. Hepatocellular carcinoma in HCV-infected patients awaiting liver transplantation: genes involved in tumor progression. *Liver Transpl.* 2004; 10:607. [PubMed: 15108252]
24. Mas VR, Maluf DG, Archer KJ, et al. Genes involved in viral carcinogenesis and tumor initiation in hepatitis C virus-induced hepatocellular carcinoma. *Mol.Med.* 2009; 15:85. [PubMed: 19098997]
25. Dumur CI, Nasim S, Best AM, et al. Evaluation of quality-control criteria for microarray gene expression analysis. *Clin.Chem.* 2004; 50:1994. [PubMed: 15364885]
26. R Development Core Team. R: A Language and Environment for Statistical Computing. Vienna, Austria: R Foundation for Statistical Computing; 2011. ISBN: 3-900051-07-0
27. Benjamini Y, Hochberg Y. Controlling the false discovery rate: A practical and powerful approach to multiple testing. *Journal of the Royal Statistical Society. Series B (Methodological).* 1995:289.
28. Gehrau RC, Mas VR, Dumur CI, et al. Regulation of molecular pathways in ischemia-reperfusion injury after liver transplantation. *Transplantation.* 2013; 96:926. [PubMed: 23985720]
29. Jaeschke H, Woolbright BL. Current strategies to minimize hepatic ischemia-reperfusion injury by targeting reactive oxygen species. *Transplant.Rev.(Orlando).* 2012; 26:103. [PubMed: 22459037]
30. Neuberger J. Transplantation: Assessment of liver allograft steatosis. *Nat.Rev.Gastroenterol.Hepatol.* 2013; 10:328. [PubMed: 23629606]

31. Noujaim HM, de Ville de Goyet J, Montero EF, et al. Expanding postmortem donor pool using steatotic liver grafts: a new look. *Transplantation*. 2009; 87:919. [PubMed: 19300197]
32. McCormack L, Dutkowski P, El-Badry AM, Clavien PA. Liver transplantation using fatty livers: always feasible? *J.Hepatol*. 2011; 54:1055. [PubMed: 21145846]
33. Chavin KD, Taber DJ, Norcross M, et al. Safe use of highly steatotic livers by utilizing a donor/recipient clinical algorithm. *Clin.Transplant*. 2013; 27:732. [PubMed: 23991646]
34. Gao XR, Adhikari CM, Peng LY, et al. Efficacy of different doses of aspirin in decreasing blood levels of inflammatory markers in patients with cardiovascular metabolic syndrome. *J.Pharm.Pharmacol*. 2009; 61:1505. [PubMed: 19903376]
35. Angele MK, Rentsch M, Hartl WH, et al. Effect of graft steatosis on liver function and organ survival after liver transplantation. *Am.J.Surg*. 2008; 195:214. [PubMed: 18154767]
36. Soejima Y, Shimada M, Suehiro T, et al. Use of steatotic graft in living-donor liver transplantation. *Transplantation*. 2003; 76:344. [PubMed: 12883190]
37. Kwon CH, Joh JW, Lee KW, et al. Safety of donors with fatty liver in liver transplantation. *Transplant.Proc*. 2006; 38:2106. [PubMed: 16980014]
38. Cho JY, Suh KS, Kwon CH, Yi NJ, Lee KU. Mild hepatic steatosis is not a major risk factor for hepatectomy and regenerative power is not impaired. *Surgery*. 2006; 139:508. [PubMed: 16627060]
39. Dutkowski P, Schlegel A, Slankamenac K, et al. The use of fatty liver grafts in modern allocation systems: risk assessment by the balance of risk (BAR) score. *Ann.Surg*. 2012; 256:861. [PubMed: 23095632]
40. Chu MJ, Vather R, Hickey AJ, Phillips AR, Bartlett AS. Impact of ischaemic preconditioning on experimental steatotic livers following hepatic ischaemia-reperfusion injury: a systematic review. *HPB (Oxford)*. 2014
41. Varela AT, Rolo AP, Palmeira CM. Fatty liver and ischemia/reperfusion: are there drugs able to mitigate injury? *Curr.Med.Chem*. 2011; 18:4987. [PubMed: 22050747]
42. Jiang X, Tian W, Sung YK, Qian J, Nicolls MR. Macrophages in solid organ transplantation. *Vasc.Cell*. 2014; 6:5. [PubMed: 24612731]
43. Weigand K, Brost S, Steinebrunner N, Buchler M, Schemmer P, Muller M. Ischemia/Reperfusion injury in liver surgery and transplantation: pathophysiology. *HPB Surg*. 2012; 2012:176723. [PubMed: 22693364]
44. Zhai Y, Qiao B, Gao F, et al. Type I, but not type II, interferon is critical in liver injury induced after ischemia and reperfusion. *Hepatology*. 2008; 47:199. [PubMed: 17935177]
45. McCoy CE, O'Neill LA. The role of toll-like receptors in macrophages. *Front.Biosci*. 2008; 13:62. [PubMed: 17981528]
46. Llacuna L, Fernandez A, Montfort CV, et al. Targeting cholesterol at different levels in the mevalonate pathway protects fatty liver against ischemia-reperfusion injury. *J.Hepatol*. 2011; 54:1002. [PubMed: 21145825]
47. Diczfalusy U, Olofsson KE, Carlsson AM, et al. Marked upregulation of cholesterol 25-hydroxylase expression by lipopolysaccharide. *J.Lipid Res*. 2009; 50:2258. [PubMed: 19502589]
48. Gold ES, Diercks AH, Podolsky I, et al. 25-Hydroxycholesterol acts as an amplifier of inflammatory signaling. *Proc.Natl.Acad.Sci.U.S.A*. 2014; 111:10666. [PubMed: 24994901]
49. Deroose JP, Kazemier G, Zondervan P, Ijzermans JN, Metselaar HJ, Alwayn IP. Hepatic steatosis is not always a contraindication for cadaveric liver transplantation. *HPB (Oxford)*. 2011; 13:417. [PubMed: 21609375]
50. Degli Esposti D, Sebah M, Pham P, et al. Ischemic preconditioning induces autophagy and limits necrosis in human recipients of fatty liver grafts, decreasing the incidence of rejection episodes. *Cell.Death Dis*. 2011; 2:e111. [PubMed: 21368883]
51. McCormack L, Petrowsky H, Jochum W, Mullhaupt B, Weber M, Clavien PA. Use of severely steatotic grafts in liver transplantation: a matched case-control study. *Ann.Surg*. 2007; 246:940. [PubMed: 18043095]
52. Yang HT, Chen KF, Lu Q, et al. Ultrasonic integrated backscatter in assessing liver steatosis before and after liver transplantation. *Hepatobiliary.Pancreat.Dis.Int*. 2014; 13:402. [PubMed: 25100125]

53. Knaak JM, Spetzler VN, Goldaracena N, Louis KS, Selzner N, Selzner M. Technique of subnormothermic ex vivo liver perfusion for the storage, assessment, and repair of marginal liver grafts. *J.Vis.Exp.* 2014
54. Berthiaume F, Barbe L, Mokuno Y, MacDonald AD, Jindal R, Yarmush ML. Steatosis reversibly increases hepatocyte sensitivity to hypoxia-reoxygenation injury. *J.Surg.Res.* 2009; 152:54. [PubMed: 18599084]
55. Oshita A, Tashiro H, Amano H, et al. Safety and feasibility of diet-treated donors with steatotic livers at the initial consultation for living-donor liver transplantation. *Transplantation.* 2012; 93:1024. [PubMed: 22495493]

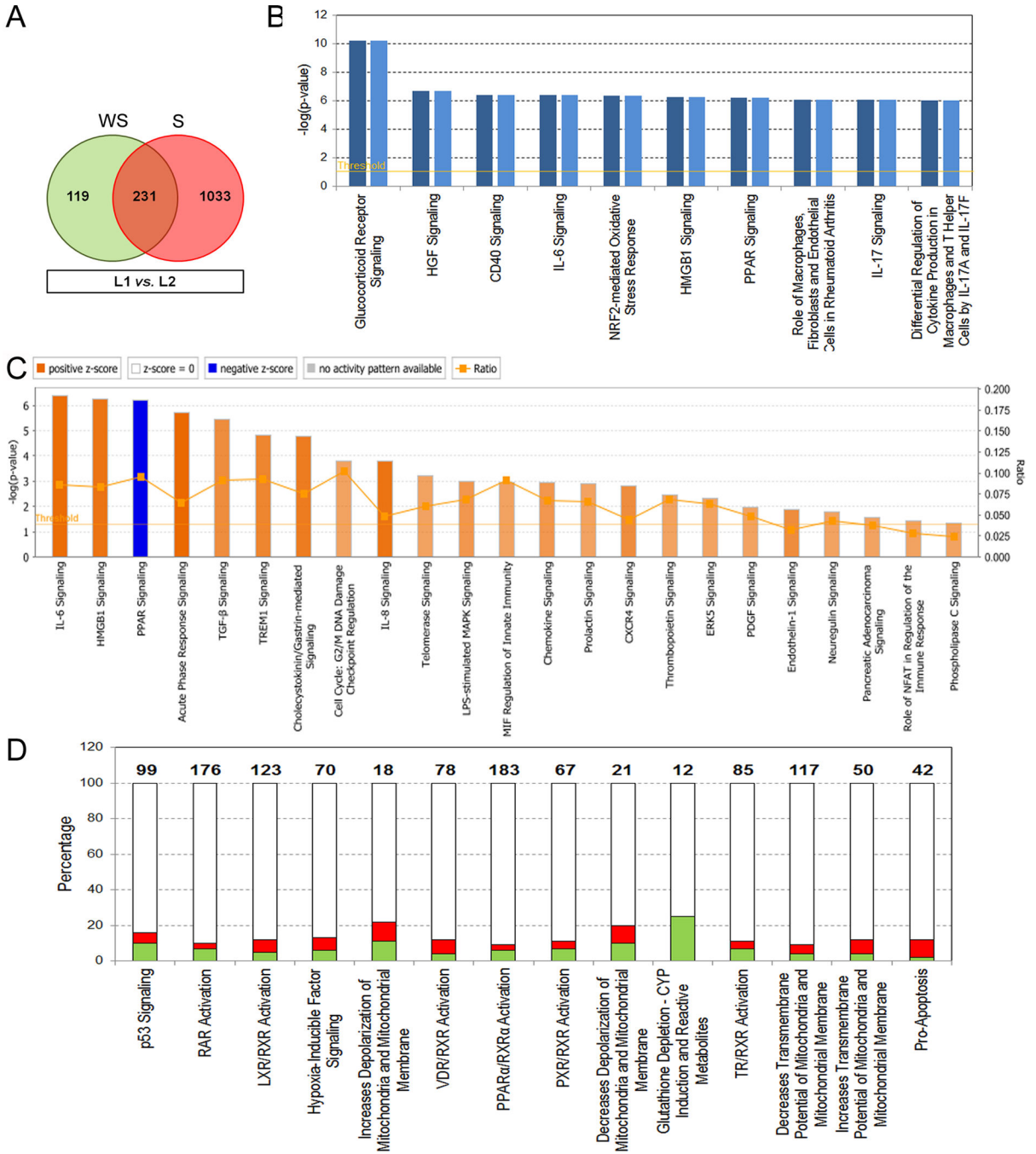


Figure 1. Differentially expressed genes and associated canonical pathways post-reperfusion in liver allografts with and without steatosis

A. Venn diagram comparing gene expression profiles between L1 vs. L2. **B.** Comparison analysis of top ten significant canonical pathways of common genes (n = 231) between study groups. Dark and light blue bars represent steatotic (S group) and no-steatotic (WS group) livers, respectively. Significance is represented by $-\log(p\text{-value})$ with threshold of 1.3 ($p = 0.05$) indicated by an orange line. **C.** Significant canonical pathways identified from common genes and with assigned z-score values to predict functional activity as inhibited

(Blue bars) or activated (Orange bars). Orange color gradient is directly proportional with grade of activation. **D.** Molecular pathways involved in damage and toxicity significantly associated with unique genes from S group. Ratios indicate the number of present molecules in the analyzed profile over the total number of molecules involved in the canonical pathway indicated on top of each bar. Red: up-regulation, Green: down-regulation. NS: no-steatosis; WS: with steatosis.

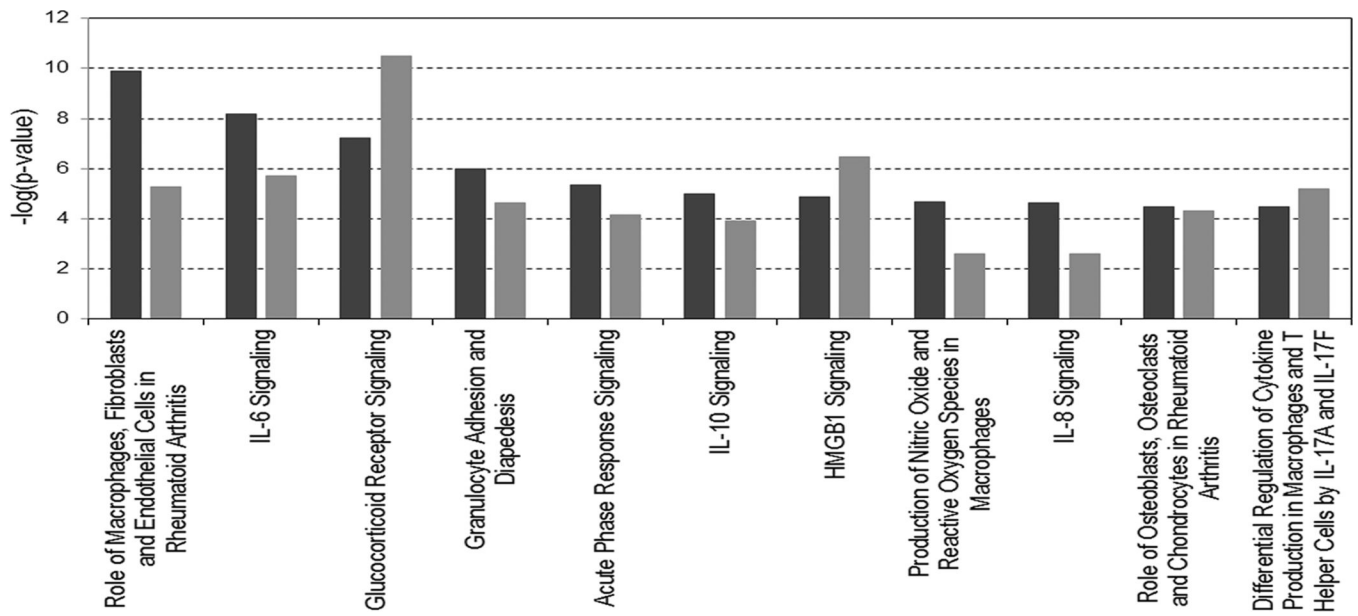


Figure 2. Comparison between groups of significant canonical pathways associated with immune and inflammatory response

Black and gray bars represent steatotic (S group) and no-steatotic (WS group) livers, respectively. Significance is represented by $-\log(p\text{-value})$.

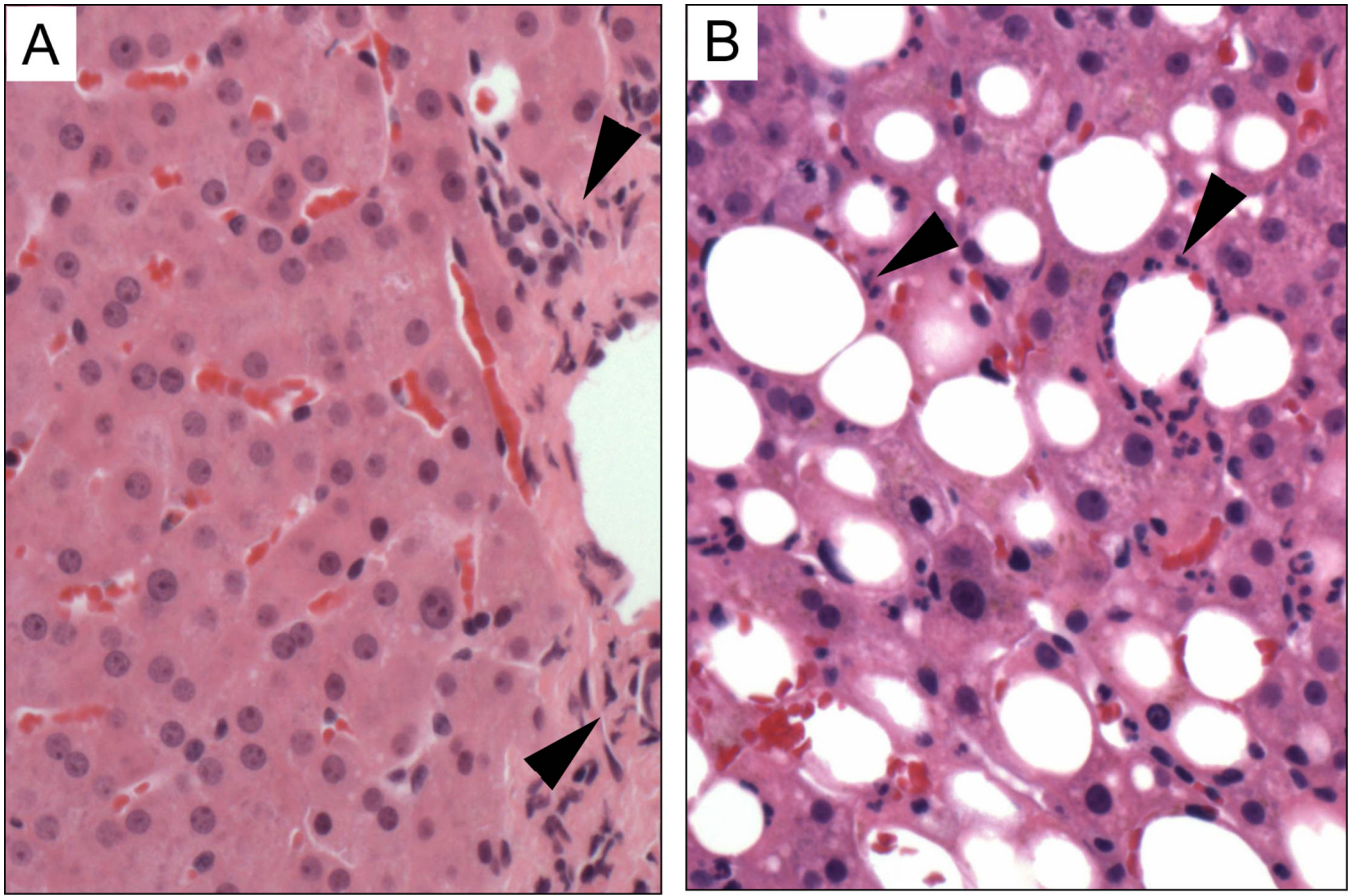


Figure 3. Histological evaluations of liver allograft infiltrates at post-reperfusion
Representative pictures of Hematoxylin & Eosin (H&E) stained allograft biopsy tissue sections. **A.** Normal non-steatotic liver (group WS) demonstrating only rare lymphocytes within a portal triad. **B.** Steatotic liver (group S) demonstrating a prominent neutrophilic infiltrate around affected area of hepatocytes accumulating lipids. Black arrow-heads indicate neutrophilic pro-inflammatory cellular infiltrates. Microscopic Magnification: 200X.

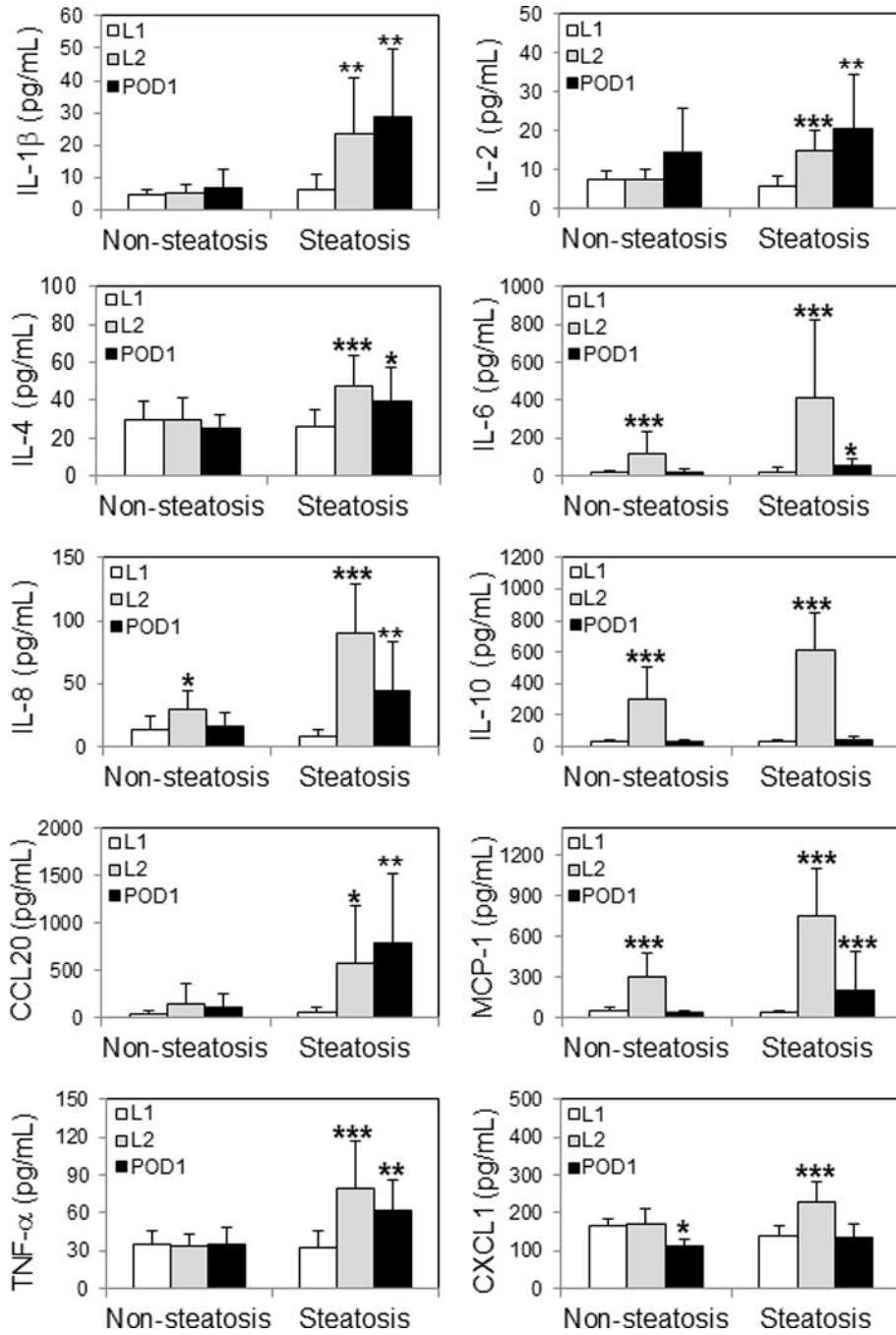


Figure 4. Circulating levels of pro-inflammatory cytokines
 Concentrations of 10 selected cytokines tested in plasma samples collected at pre-implantation (L1), post-reperfusion (L2), and 1-day post-surgery (POD1) from LT recipients of non-steatotic and steatotic grafts are shown individually. Statistical analyses were performed between L1 vs. L2 and L1 vs. POD1 for each group. Significant p-values are indicated: * $p < 0.05$; ** $p < 0.01$; *** $p < 0.001$.

Table 1

Characteristics of the cohort of patients

A Demographics and clinical parameters			
Study groups	WS (n = 13)	S (n = 17)	p-value
Recipient			
Age (years)	X ± SD	55 ± 7.9	0.122
Gender, n (%)	Male	12 (71)	0.327
	Female	5 (29)	
Race, n (%)	Caucasian	11 (66)	0.069
	African-American	2 (12)	
	Other	4 (24)	
End stage of liver disease etiology, n (%)	Hepatitis C	5 (29)	0.045
	Alcohol	3 (18)	
	NASH	0 (0)	
	Other*	5 (39)	
MELD (Tx)	X ± SD	25.0 ± 4.0	0.630
Waitlist time (days)	X ± SD	537 ± 900	0.268
Life status, n (%)	Alive	12 (71)	0.321
	Deceased	1 (8)	
Hospital length-of-stay (days)	X ± SD	14 ± 11	0.628
Donor			
Age (years)	Years	49 ± 13	0.209
Gender, n (%)	Male	9 (53)	0.920
	Female	8 (47)	
Race, n (%)	Caucasian	14 (82)	0.318
	African-American	3 (18)	
	Other	0 (0)	
Vasopressors	Yes	10 (59)	0.751
	No	7 (41)	

A Demographics and clinical parameters				
Study groups		WS (n = 13)	S (n = 17)	p-value
Allograft				
CIT (hours)	X ± SD	6.0 ± 1.5	7.0 ± 1.9	0.077
WIT (minutes)	X ± SD	33 ± 12	32 ± 15	0.761
Steatosis (%)	X ± SD	2.6 ± 1	28 ± 3	< 0.001

B Biochemical parameters					
Study groups	Parameter	Time-point	WS (n = 13)	S (n = 17)	p-value
AST	IU/L (X ± SD)	pre-LT	73 ± 49	92 ± 62	0.469
		post-LT	578 ± 204	2696 ± 1732	<0.001
		POD 1	367 ± 271	1019 ± 715	0.011
		POD 7	53 ± 76	76 ± 66	0.320
		1 month	49 ± 82	57 ± 52	0.857
ALT	IU/L (X ± SD)	pre-LT	44 ± 46	81 ± 94	0.227
		post-LT	358 ± 213	1235 ± 1015	0.009
		POD 1	295 ± 221	686 ± 481	0.023
		POD 7	99 ± 77	179 ± 100	0.018
		1 month	54 ± 73	102 ± 143	0.411
Total Bilirubin	mg/dL (X ± SD)	pre-LT	8.8 ± 8.8	8.8 ± 8.5	0.930
		post-LT	6.0 ± 5.5	5.9 ± 2.6	0.854
		POD 1	4.4 ± 4.0	5.1 ± 3.2	0.722
		POD 7	2.4 ± 2.0	4.6 ± 5.0	0.191
		1 month	1.2 ± 1.0	6.6 ± 10.3	0.149
INR	(X ± SD)	pre-LT	2.0 ± 0.6	1.8 ± 0.8	0.522
		post-LT	2.0 ± 0.6	2.0 ± 0.5	0.840
		POD 1	1.6 ± 0.4	1.6 ± 0.3	0.809
		POD 7	1.4 ± 0.4	1.3 ± 0.3	0.566
		1 month	1.5 ± 0.7	1.5 ± 0.8	0.967

Author Manuscript

Author Manuscript

Author Manuscript

Author Manuscript

* Other: Cryptogenic cirrhosis, Primary Sclerosis Cholangitis without or with colangiocarcinoma (PSC or PSC/CCA), Hepatitis B, Autoimmune Hepatitis, X: average; SD: standard deviation; CIT: cold-ischemia time; WIT: warm-ischemia time.

WS: Without Steatosis; S: With Steatosis; AST: Aspartate Aminotransferase; ALT: Alanine Aminotransferase; INR: International Normalized Ratio; POD: Post-Operative Day; X: average value; SD: Standard Deviation.

Table 2

Associated network functions for WS and S groups unique genes.

A S group unique genes top ten associated network functions.		
Top Diseases and Functions	Score	Focus Molecules
Connective Tissue Disorders, Developmental Disorder, Hematological Disease	50	33
Cancer, Hereditary Disorder, Neurological Disease	50	35
Embryonic Development, Organismal Development, Tissue Development	42	30
Developmental Disorder, Hereditary Disorder, Neurological Disease	42	32
Cancer, Cellular Movement, Tumor Morphology	42	31
Cell Morphology, Cellular Function and Maintenance, Connective Tissue Development and Function	39	31
Cell Morphology, Cellular Assembly and Organization, Cellular Function and Maintenance	39	28
Behavior, Nervous System Development and Function, Hereditary Disorder	39	31
DNA Replication, Recombination, and Repair, Cancer, Dermatological Diseases and Conditions	37	30
Molecular Transport, RNA Trafficking, Connective Tissue Development and Function	35	29

B Associated network function in WS liver allografts unique genes.		
Top Diseases and Functions	Score	Focus Molecules
Connective Tissue Development and Function, Tissue Development, Cellular Compromise	36	19
Cell Morphology, Cellular Development, Cellular Growth and Proliferation	34	18
Cancer, Amino Acid Metabolism, Molecular Transport	34	22
Cell Morphology, Nervous System Development and Function, Tissue Morphology	29	18
Cancer, Gastrointestinal Disease, Developmental Disorder	22	14
Cellular Assembly and Organization, Digestive System Development and Function, Embryonic Development	20	12
Cellular Development, Embryonic Development, Organismal Development	18	14
Dermatological Diseases and Conditions, Immunological Disease, Gastrointestinal Disease	16	10

Table 3

Predicted activity of disease and biological functions in S and WS groups

Diseases and Biological Functions	S group	WS group
Recruitment of blood cells	3.5	
Recruitment of granulocytes	3.0	
migration of blood cells	2.7	
Cell movement of blood cells	2.7	
Accumulation of myeloid cells	2.4	
Immune response of leukocytes	2.3	
Cell movement of lymphocytes		3.6
Cell movement of mononuclear leukocytes		3.6
Activation of antigen presenting cells		3.4
Adhesion of immune cells		3.0
Mobilization of leukocytes		2.8
Adhesion of blood cells		2.7
Migration of phagocytes		2.5
Recruitment of antigen presenting cells		2.2
Recruitment of lymphocytes		2.1
Recruitment of T lymphocytes		2.0
Induction of leukocytes		2.0
Recruitment of cells	3.7	3.7
Homing of cells	3.6	2.9
Homing	3.5	2.9
Recruitment of leukocytes	3.4	3.3
Recruitment of phagocytes	3.2	2.9
Recruitment of neutrophils	2.8	2.6
Cell movement of leukocytes	2.8	3.1
Leukocyte migration	2.7	3.1
Activation of phagocytes	2.6	3.4
Cell movement of myeloid cells	2.6	2.5
Accumulation of leukocytes	2.4	2.3
Inflammatory response	2.3	2.4
Cell movement of phagocytes	2.1	2.6
Cell movement of antigen presenting cells	1.8	2.3
Differentiation of blood cells	1.6	2.1
Differentiation of leukocytes	1.2	2.0
Activation of leukocytes	1.0	2.2
Homeostasis of leukocytes	0.8	2.0
Development of lymphocytes	0.6	2.0
Lymphocyte homeostasis	0.6	2.0

Diseases and Biological Functions	S group	WS group
T cell homeostasis	0.3	2.0
T cell development	0.3	2.3

Numbers indicate z-scores. Z-scores equal or higher than 2.0 are considered significant.

Author Manuscript

Author Manuscript

Author Manuscript

Author Manuscript

Table 4

Validation analysis of S group selected genes

Gene ID	Gene Name	Microarray data L1 vs. L2 (FC)	p-value	Taqman RT-PCR L1 vs. L2 (FC)	p-value
CH25H	Cholesterol 25-hydroxylase	8.6	7.6E-08	9.6	2.1E-06
EGR3	Early growth response 3	4.5	3.8E-05	12.6	1.5E-04
SOC33	Suppressor of cytokine signaling 3	3.5	5.5E-08	13.0	7.5E-06
CCL2	Chemokine (C-C motif) ligand 2	5.3	1.1E-05	10.1	2.5E-05
TNFAIP6	Tumor necrosis factor, alpha-induced protein 6	4.3	9.9E-05	10.0	2.3E-04

FC: Fold-change

Table 5
Comparison analysis of circulating cytokines between groups at each time-point

Cytokine	L1		L2		PODI	
	S vs. WS (FC)	p-value	S vs. WS (FC)	p-value	S vs. WS (FC)	p-value
IL-1 β	1.3	0.373	4.6	0.003	4.2	0.002
IL-2	0.8	0.078	2.0	<0.0001	1.4	0.257
IL-4	0.9	0.354	1.6	0.008	1.6	0.023
IL-6	1.1	0.854	3.5	<0.0001	2.5	0.016
IL-8	0.6	0.157	3.1	<0.0001	2.7	0.022
IL-10	0.9	0.785	2.0	0.006	1.5	0.081
CCL20	1.3	0.418	4.0	0.030	6.8	0.005
MCP-1	0.8	0.261	2.5	0.002	5.5	0.073
TNF- α	0.9	0.608	2.3	0.001	1.8	0.004
CXCL1	0.9	0.068	1.4	0.008	1.2	0.039

FC: Fold-change